Variations in apparent diffusion coefficient values following chemotherapy in pediatric neuroblastoma

Senay Demir, Naime Altinkaya, Nazim Emrah Kocer, Ayse Erbay, Pelin Oguzkurt

PURPOSE
In children the assessment of solid tumors' response to chemotherapy is based primarily on size reduction, which can be unreliable and a late marker, in the presence of necrosis. We aimed to establish whether apparent diffusion coefficient (ADC) values of childhood neuroblastomas show proportional changes in relation to chemotherapy response.

METHODS
We evaluated 15 pediatric patients with abdominopelvic neuroblastomas, who had undergone MRI before and after chemotherapy. Two radiologists retrospectively analyzed all images by drawing a round uniform region-of-interest in the solid/contrast-enhancing portion of the lesions in consensus. The ADC values from pre- and postchemotherapy images were compared.

RESULTS
Postchemotherapy ADC values were significantly higher than those obtained before treatment ($P < 0.05$, for minimum, maximum, and median ADC values).

CONCLUSION
Our results support diffusion-weighted MRI as a promising noninvasive biomarker of therapeutic responses. To the best of our knowledge, this is the first report to compare diffusion-weighted imaging findings before and after chemotherapy in childhood neuroblastic tumors.

Diffusion-weighted (DW) magnetic resonance imaging (MRI) enables tracking of water molecules (Brownian motion) at a microscopic level. The use of different b values allows for the quantification of signal loss in diffusion-sensitive sequences through apparent diffusion coefficient (ADC) maps. It has been shown that highly cellular areas with restricted diffusion demonstrate low ADC values compared to areas with less cellular content. Recent technological advances, including echo-planar imaging, multichannel coils, and parallel imaging, allow for the usage of DW-MRI beyond neurological applications (1–5). The ADC values of malignant masses are relatively lower than those of benign masses, although overlapping ADC values of malignant and benign lesions have also been reported (1, 6–12). Currently, in children the assessment of solid tumors' response to chemotherapy is based on size reduction; but this method can be unreliable as a marker, as tumors that shrink substantially may still be composed mainly of malignant cells (13, 14).

Here, we aimed to evaluate whether ADC values in viable portions of childhood neuroblastomas show any changes depending on tumor cellularity before and after chemotherapy. We hypothesized that an increase in ADC values over the course of chemotherapy could be used as a noninvasive marker of therapy response. To the best of our knowledge, this is the first report to compare DW-MRI findings before and after chemotherapy in childhood neuroblastic tumors.

Methods

Patients

We retrospectively screened pediatric patients who had neuroblastic tumors and received treatment at our hospital between January 2009 and August 2013. We found 36 pediatric patients who underwent routine protocol-driven MRI assessment for solid tumors. Out of this group we acquired data from children who had intra-abdominal neuroblastic tumors that were diagnosed histopathologically. Our institution generally prefers MRI over computed tomography; however, due to capacity and time restrictions, not all patients undergo MRI both at primary diagnosis and at postchemotherapy follow-up. Only those patients who underwent MRI before and after chemotherapy were included in this study. In addition, exclusion criteria included any oncological (chemotherapy or radiotherapy) or surgical treatment before initial imaging. Consequently, we evaluated 15 patients between 4–138 months of age (mean, 37.8 months) including five females and 10 males. Thirteen patients were Stage 4 and two patients were Stage 3. The timing of scans was determined by our pediatric oncology department and all patients

From the Departments of Radiology (S.D. ✉ drsenaydemir@hotmail.com, N.A.); Pathology (N.E.K.); Pediatric Oncology (A.E.); Pediatric Surgery (P.O.), Baskent University School of Medicine, Adana, Turkey.
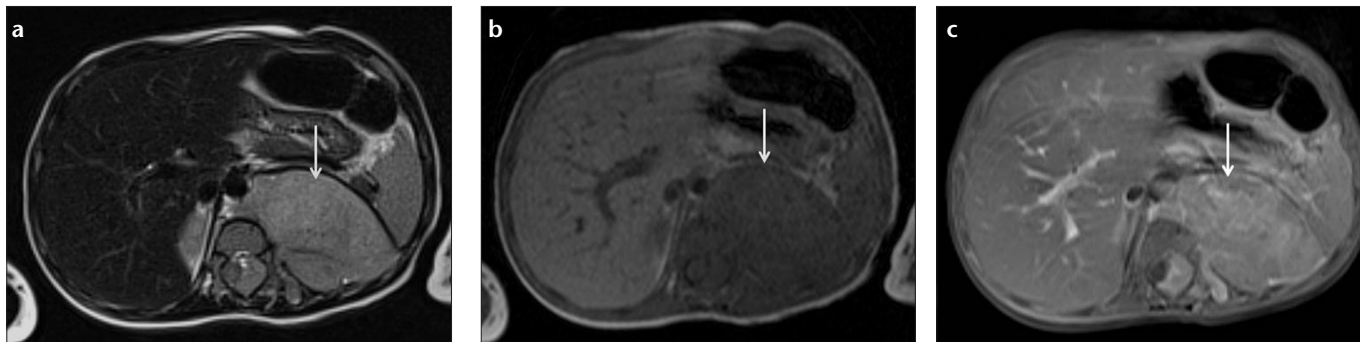
Figure 1. a–c. Axial T2-weighted **(a)**, precontrast **(b)**, and postcontrast **(c)** T1-weighted images showing the solid portion of a left-sided paravertebral ganglioneuroblastoma *(arrow)*.

in this group received chemotherapy according to relevant oncological treatment protocols. The lesions became calcified, totally hemorrhagic, or necrotic in four patients after chemotherapy and we could not obtain acceptable ADC values for these lesions. Thus, we compared pre- and postchemotherapy ADC values of 11 patients.

This study was approved by the Institutional Review Board of our university hospital (Project no:K12/121) and supported by the university research fund.

DW-MRI technique

The MRI examinations were performed on one of two Siemens 1.5 T MRI scanners (Symphony or Avanto, Siemens Healthcare) with a body or head-neck coil (depending on the child's body size). Children under seven years of age were sedated prior to the scan without intubation following an anesthesiological safety assessment that adhered to our institutional policies. All patients had peripheral or central venous access. Our routine abdominal MRI protocol included axial and coronal T2-weighted turbo spin echo (TSE) sequence (repetition time/echo time (TR/TE), 4000/103; slice thickness, 5 mm; number of excitations, 1; TSE factor, 29), precontrast axial and coronal T1-weighted fast low-angle shot (FLASH) sequence (TR/TE, 127/3.52; flip angle, 70°; slice thickness, 5 mm; number of excitations, 1), axial fat saturated T2-weighted TSE sequence (TR/TE, 4400/103; slice thickness, 5 mm; number of excitations, 1; TSE factor, 29), axial in-phase/out-of-phase imaging (TR/TE, 100/2.38–4.89; slice thickness, 5 mm; flip angle, 70°; number of excitations, 1), coronal

true fast imaging with steady-state-free precession (3D true FISP)(TR/TE= 3.79/1.57; slice thickness, 5 mm; number of excitations, 1) sequences, and contrast-enhanced axial and coronal T1-weighted sequences following a bolus injection of 0.2 mmol/kg of meglumine gadoterate (Dotarem). Respiratory triggering was used for children who were not capable of holding their breath. The mean time of the conventional MRI examination was approximately 30 min.

DW-MRI was performed before contrast medium administration and a fat-saturated pulse was used to exclude severe chemical shift artifacts. Images were obtained in the axial plane using non-breath-hold, single-shot spin-echo sequencing with the following image parameters: TR/TE, 4600/88; slice thickness, 5 mm; intersection gap, 1 mm; echo-planar readout matrix, 192×113; bandwidth, 1736 Hz/pixel. Four DW sequences were acquired to use signal averaging with b values of 0, 200, 600, 800, and 1000 s/mm², and isotropic images were generated on a pixel-by-pixel basis. ADC maps were created automatically. The mean time of the DW-MRI examination was approximately 5 min.

Image analysis

All images were analyzed retrospectively by two radiologists, one with six years of experience in pediatric imaging (S.D.) and a second with five years of experience in abdominal imaging (N.A.), using the Advantage Workstation 4.4 (GE Healthcare). We did not attempt masking because it was noticeable on the images whether they had been acquired before or after chemo-

therapy. Two readers reviewed the images in consensus and ADC measurements were made by drawing a round, 25 mm² region-of-interest (ROI). All ROIs for each lesion were placed over the solid/contrast-enhancing portion of the lesion at different slices through the tumor, which had apparent diffusion-restriction visually on the DW images. Exclusion of necrotic areas was based on T2- and contrast-enhanced T1-weighted images (Fig. 1). The ADC measurements were repeated five times at different sites and averaged. The same procedure was repeated using the images acquired after the chemotherapy and pre- and postchemotherapy images were compared. The duration between the examinations was 4–8 months (mean, 4.8 months). In the pre- and postchemotherapy series, the ROIs were not at the same exact sites due to volume decreases. Examples of ROIs drawn on pre- and postchemotherapy ADC map images of a right adrenal neuroblastoma are shown in Fig. 2.

We also measured the widest axial and craniocaudal diameters of the lesions on the images before and after chemotherapy and calculated the tumor volumes using the ellipsoid formula: length×breadth×depth×0.479.

Histopathology

Our consultant histopathologist (N.E.K., five years of experience with pediatric tumor histopathology) who was blinded to the MRI findings, reviewed histological slices from surgically resected tumors and graded their chemotherapy-induced changes as minimal, good, or marked according to current practice, considering the
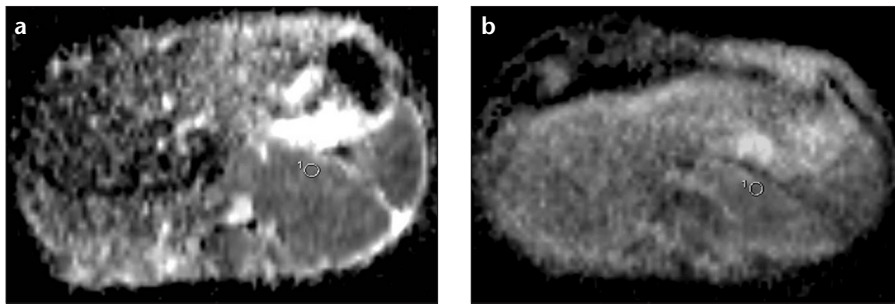
Figure 2. a, b. An example of a region-of-interest drawn on an ADC map of a ganglioneuroblastoma before **(a)** and after chemotherapy **(b)**. The mean ADC values were measured as 0.95×10^{-3} mm²/s and 1.42×10^{-3} mm²/s, respectively.

percentage of necrosis, fibrosis, and calcification that they have (13). In addition, slices were graded according to their cellularity (low, 300 cells per high power fields [HPF]; intermediate, 300–600 cells per HPF; high, 600 cells per HPF; intermixed, variable cellularity) (15).

Three postchemotherapy specimens were obtained with tru-cut biopsy and excluded from this assessment. One patient was operated at another institution after chemotherapy and we could not evaluate the specimen. Prechemotherapy specimens were mostly obtained with tru-cut or from bone marrow, so they were not subject to comparison with postchemotherapy specimens in terms of cellularity.

Statistical analysis

Statistical analysis was performed using the Statistical Package for Social Sciences version 17.0 (SPSS for Windows, SPSS Inc.). Data were described as median because the continuous variables were not normally distributed ($P > 0.05$ in Kolmogorov-Smirnov test or Shapiro-Wilk, if n<30). Comparisons of not normally distributed data from pre- and postchemotherapy images were analyzed using the Wilcoxon test. $P < 0.05$ was considered statistically significant.

Results

We evaluated 15 pediatric patients (10 males and five females) with abdominopelvic neuroblastic tumors, having 4–138 months of age (mean, 37.8 months). Twelve of the lesions were located on an adrenal site and mostly accompanied by lymphadenopathy. Two patients had para-aortic/paravertebral lesions. One lesion was located in the presacral region and was pathologically shown to be a ganglioneuroblastoma (Table 1).

We could not obtain acceptable ADC values in four patients after chemotherapy because the lesions became calcified, totally hemorrhagic, or necrotic. We failed to find a contrast enhancing region to draw a ROI in these patients' lesions. Thus, we compared the pre- and postchemotherapy ADC values of 11 patients.

Before chemotherapy, the mean ADC values of the neuroblastomas and ganglioneuroblastomas in 15 patients ranged between 0.54×10^{-3} mm²/s and 1.17×10^{-3} mm²/s (median, 0.74×10^{-3} mm²/s). After chemotherapy, in 11 patients, the mean ADC values of the lesions ranged between 0.70×10^{-3} mm²/s and 1.25×10^{-3} mm²/s (median, 1.05×10^{-3} mm²/s). Postchemotherapy ADC values in these 11 patients were significantly higher than those obtained before treatment ($P = 0.003$). Table 1 summarizes data on lesion location, histopathological diagnosis, volume, pre- and postchemotherapy ADC values, and grading of chemotherapy-induced responses. Pre- and postchemotherapy ADC measurements of 11 patients is shown in Table 2. At the onset of our follow-up, the volume of the smallest lesion was 7 mL and the largest was 1250 mL. After chemotherapy, the mean volume of all lesions decreased by 88% (from 281.9 mL to 36.4 mL). There was no significant correlation between the size reduction of the lesions and the increase in the ADC values. Also, there was no significant relationship between the ADC values of the lesions after chemotherapy and their cellularity rates after resection.

Discussion

In this study we found an increased distribution of ADC values after chemotherapy in 11 patients. The median of the ADC values of all lesions increased from 0.74×10^{-3} mm²/s to 1.05×10^{-3} mm²/s postchemotherapy. All lesions showed volume loss after chemotherapy except for the smallest lesion (patient 14), which showed no volume loss despite minimal increase in ADC value postchemotherapy.

To the best of our knowledge, this is the first report to compare pre- and postchemotherapy DW-MRI findings in pediatric neuroblastic tumors. In 2002, Uhl at al. (16) reported the first results on DW-MRI in neuroblastomas with correlations to histology. Since then, there have been few reports on DW-MRI for pediatric abdominal tumors (7). Kocaoglu et al. (1) described 31 abdominal masses, 15 of which were malignant, and proposed an ADC value of 1.1×10^{-3} mm²/s as a cutoff value to differentiate malignant from benign masses. In 2011, McDonald et al. (13) reported a shift in the distribution of ADC patterns of pediatric abdominal tumors during chemotherapy. In the present study, we included a group of childhood neuroblastoma cases to investigate the correlation between chemotherapy response and reduction of diffusion restriction in neuroblastic tumors. In our series the increase in ADC values was not proportional to the volume loss of the tumors.

Humphries et al. (12) reported a correlation between ADC value and tumor cellularity in pediatric patients. Prechemotherapy specimens of our patients were mostly obtained with tru-cut or from bone marrow; thus, we could not evaluate the relationship between their cellularity and ADC values or compare them with postchemotherapy specimens in terms of cellularity. We could not demonstrate a significant relationship between the ADC values of the lesions after chemotherapy and their cellularity rates after resection. The ADC increase after chemotherapy seemed to be proportional with the rate of chemotherapy-induced histopathological changes, but the patient numbers were not adequate to prove a statistically significant relation. We accept that this is

Table 1. Summary of patient history and pre- and postchemotherapy findings by MRI and histopathology

Patient no.	Age (months)/ gender	Diagnosis/ location	Prechemotherapy		Postchemotherapy		Interval between exams (months)	Histopathologic response
			Mass volume (mL)	Mean and range of ADC ($\times 10^{-3}$ mm^2/s)	Mass volume (mL)	Mean and range of ADC ($\times 10^{-3}$ mm^2/s)		
1	46/M	Neuroblastoma/ left adrenal	105	0.84 (0.68–1.03)	10	(Necrotic)	5	Marked
2	19/F	Neuroblastoma/ right adrenal	490	0.74 (0.62–0.91)	33	1.05 (0.80–1.33)	6	Good
3	18/F	Neuroblastoma/ left adrenal	1250	0.71 (0.60–0.92)	44	0.80 (0.71–0.92)	8	Minimal
4	25/M	Ganglioneuroblastoma/ left adrenal	45	0.78 (0.71–0.86)	9	0.86 (0.77–0.99)	5	Minimal
5	34/M	Neuroblastoma/ right adrenal	478	0.61 (0.49–0.76)	12	0.70 (0.65–0.75)	4	Good
6	11/M	Neuroblastoma/ para-aortic	345	0.72 (0.66–0.81)	26	1.09 (1.01–1.22)	4	Tru-cut
7	62/M	Ganglioneuroblastoma/ left adrenal	150	0.54 (0.47–0.60)	40	1.25 (1.12–1.36)	5	N/A
8	138/F	Ganglioneuroblastoma/ presacral	182	0.72 (0.66–0.77)	90	0.81 (0.74–0.93)	5	Minimal
9	40/M	Neuroblastoma/left adrenal-para-aortic	140	0.60 (0.51–0.71)	10	(Hemorrhagic)	4	Marked
10	96/M	Neuroblastoma/ left adrenal	460	0.87 (0.70–1.01)	70	0.95 (0.83–1.02)	5	Minimal
11	4/M	Neuroblastoma/ left adrenal	15	1.17 (0.87–1.52)	8	(Hemorrhagic and calcified)	5	Marked
12	12/F	Neuroblastoma/ right adrenal	286	0.79 (0.64–0.97)	78	(Necrotic and calcified)	5	Tru-cut
13	5/M	Neuroblastoma/ right adrenal	78	0.58 (0.54–0.64)	12	1.13 (1.04–1.23)	3	Marked
14	31/M	Neuroblastoma/ right adrenal	7	1.14 (1.12–1.21)	7	1.21 (0.96–1.35)	4	Tru-cut
15	26/F	Ganglioneuroblastoma/ paravertebral	198	0.79 (0.74–0.85)	98	1.20 (1.06–1.29)	4	Good
Mean (±SD)	37.8		281.9	0.77 (±0.18)	36.4	1.00 (±0.19)	4.8	

ADC, apparent diffusion coefficient; M, male; F, female; N/A, not available (no postchemotherapy specimen); SD, standard deviation.

Table 2. Comparison of pre- and postchemotherapy ADC measurements of 11 patients

ADC	Median	Min–max
Prechemotherapy	0.74	0.54–1.17
Postchemotherapy	1.05	0.70–1.25

$P = 0.003$.
ADC, apparent diffusion coefficient.

a feasibility study with a relatively small number of observations. As indicated in previous studies, our findings suggest a correlation between ADC distribution and biological response to chemotherapy (12,13,17–21).

Previous studies have shown that tumor shrinkage might be a delayed or insensitive marker (in case of partial response) to evaluate chemotherapy response; absence of reduction in tumor size does not necessarily mean no response (13, 14, 22). Particularly for solid, viable tumors, new methods are needed to histopathologically detect a lack of chemotherapy response in a shrinking tumor or the degree of response in a growing tumor. We trust that our findings will contribute towards establishing a supplemental method for this purpose.

In the literature, some investigators used large ROIs that included most solid parts of the lesions (6, 13); however, we preferred round, 25 mm^2 ROIs placed around the solid/contrast-enhancing portion with restricted visual diffusion, and averaged the results which, we believe, is a good method to exclude cystic parts, vessels, normal parenchyma, and areas with unclear intensities due to calcification or motion artifacts.

There were some limitations to this study. First, the long intervals between pre- and post-treatment MRI investigations prevented us from concluding precisely that chemotherapy is the only factor causing the increase in ADC values. Second, we could not differentiate ganglioneuroblastomas from neuroblastomas, based on ADC values before or after chemotherapy, because of the insufficient number of ganglioneuroblastoma cases. Gahr et al. (6) also reported that ADC values are related to the histopathological aspect of a tumor but cannot be used to differentiate a neuroblastoma from a ganglioneuroblastoma/ganglioneuroma yet.

In conclusion, our results support the opinion that ADC values change after chemotherapy and can provide promising evidence to assess chemotherapy response in pediatric neuroblastic tumors. We observed increased ADC values in viable parts of childhood abdominal neuroblastomas after chemotherapy. If verified in larger series, DW-MRI may be a promising noninvasive biomarker and can aid in the assessment of therapeutic responses.

Conflict of interest disclosure

The authors declared no conflicts of interest.

References

1. Kocaoglu M, Bulakbasi N, Sanal HT, et al. Pediatric abdominal masses: diagnostic accuracy of diffusion weighted MRI. Magn Reson Imaging 2010; 28:629–636. [CrossRef]
2. Szafer A, Zhong J, Gore JC. Theoretical model for water diffusion in tissues. Magn Reson Med 1995; 33:697–712. [CrossRef]
3. Colagrande S, Belli G, Politi LS, Mannelli L, Pasquinelli F, Villari N. The influence of diffusion- and relaxation-related factors on signal intensity: an introductive guide to magnetic resonance diffusion-weighted imaging studies. J Comput Assist Tomogr 2008; 32:463–474. [CrossRef]
4. Turkbey B, Aras O, Karabulut N, et al. Diffusion-weighted MRI for detecting and monitoring cancer: a review of current applications in body imaging. Diagn Interv Radiol 2012; 18:46–59. [CrossRef]
5. Koh DM, Collins DJ. Diffusion-weighted MRI in the body: applications and challenges in oncology. AJR Am J Roentgenol 2007; 188:1622–1635. [CrossRef]
6. Gahr N, Darge K, Hahn G, Kreher BW, von Buiren M, Uhl M. Diffusion-weighted MRI for differentiation of neuroblastoma and ganglioneuroblastoma/ganglioneuroma. Eur J Radiol 2011; 79:443–446. [CrossRef]
7. Battal B, Akgun V, Kocaoglu M. Diffusion weighted MRI beyond the central nervous system in children. Diagn Interv Radiol 2012; 18:288–297. [CrossRef]
8. MacKenzie JD, Gonzalez L, Hernandez A, Ruppert K, Jaramillo D. Diffusion-weighted and diffusion tensor imaging for pediatric musculoskeletal disorders. Pediatr Radiol 2007; 37:781–788. [CrossRef]
9. Abdel Razek AA, Gaballa G, Elhawarey G, Elshafey M, Elhadedy T. Characterization of pediatric head and neck masses with diffusion-weighted MR imaging. Eur Radiol 2009; 19:201–208. [CrossRef]
10. Alibek S, Cavallaro A, Aplas A, Uder M, Staatz G. Diffusion weighted imaging of pediatric and adolescent malignancies with regard to detection and delineation: initial experience. Acad Radiol 2009; 16:866–871. [CrossRef]
11. Abdel Razek AA, Soliman N, Elashery. R. Apparent diffusion coefficient values of mediastinal masses in children. Eur J Radiol 2011; 81:1311–1314. [CrossRef]
12. Humphries PD, Sebire NJ, Siegel MJ, Olsen ØE. Tumors in pediatric patients at diffusion-weighted MR imaging: apparent diffusion coefficient and tumor cellularity. Radiology 2007; 245:848–854. [CrossRef]
13. McDonald K, Sebire NJ, Anderson J, Olsen ØE. Patterns of shift in ADC distributions in abdominal tumours during chemotherapy—feasibility study. Pediatr Radiol 2011; 41:99–106. [CrossRef]
14. Olsen ØE, Jeanes AC, Sebire NJ, et al. Changes in computed tomography features following preoperative chemotherapy for nephroblastoma: relation to histopathological classification. Eur Radiol 2004; 14:990–994. [CrossRef]
15. Ambros IM, Hata J, Joshi VV, et al. Morphologic features of neuroblastoma (Schwannian stroma-poor tumors) in clinically favorable and unfavorable groups. Cancer 2002; 94:1574–83. [CrossRef]
16. Uhl M, Altehoefer C, Kontny U, Ilyasov K, Buchert M, Langer M. MRI-diffusion imaging of neuroblastomas: first results and correlation to histology. Eur Radiol 2002; 12:2335–2338. [CrossRef]
17. Kauppinen RA. Monitoring cytotoxic tumour treatment response by diffusion magnetic resonance imaging and proton spectroscopy. NMR Biomed 2002; 15:6–17. [CrossRef]
18. Uhl M, Saueressig U, van Buiren M, et al. Osteosarcoma: preliminary results of in vivo assessment of tumour necrosis after chemotherapy with diffusion- and perfusion-weighted magnetic resonance imaging. Invest Radiol 2006; 41:618–623. [CrossRef]
19. Erlemann R, Sciuk J, Bosse A, et al. Response of osteosarcoma and Ewing sarcoma to preoperative chemotherapy: assessment with dynamic and static MR imaging and skeletal scintigraphy. Radiology 1990; 175:791–796. [CrossRef]
20. Ross BD, Moffat BA, Lawrence TS, et al. Evaluation of cancer therapy using diffusion magnetic resonance imaging. Mol Cancer Ther 2003; 2:581–587.
21. Kotsenas AL, Roth TC, Manness WK, Faerber EN. Abnormal diffusion-weighted MRI in medulloblastoma: does it reflect small cell histology? Pediatr Radiol 1990; 29:524–526. [CrossRef]
22. Anderson J, Slater O, McHugh K, et al. Response without shrinkage in bilateral Wilms tumor: significance of rhabdomyomatous histology. J Pediatr Hematol Oncol 2002; 24:31–34. [CrossRef]